

# PROCEEDINGS OF SPIE

[SPIDigitalLibrary.org/conference-proceedings-of-spie](https://spiedigitallibrary.org/conference-proceedings-of-spie)

## Height distributions of uncapped InAs/InGaAsP/InP quantum dashes and their effect on emission wavelengths

Obhi, Ras-Jeevan, Schaefer, Sebastian, Valdivia, Christopher, Poole, Philip, Liu, Jiaren, et al.

Ras-Jeevan K. Obhi, Sebastian W. Schaefer, Christopher E. Valdivia, Philip J. Poole, Jiaren Liu, Zhenguo Lu, Karin Hinzer, "Height distributions of uncapped InAs/InGaAsP/InP quantum dashes and their effect on emission wavelengths," Proc. SPIE 12010, Photonic and Phononic Properties of Engineered Nanostructures XII, 120100C (5 March 2022); doi: 10.1117/12.2609954

**SPIE.**

Event: SPIE OPTO, 2022, San Francisco, California, United States

# Height Distributions of Uncapped InAs/InGaAsP/InP Quantum Dashes and Their Effect on Emission Wavelengths

Ras-Jeevan K. Obhi<sup>\*a</sup>, Sebastian W. Schaefer<sup>a</sup>, Christopher E. Valdivia<sup>a</sup>, Philip J. Poole<sup>b</sup>,  
Jiaren Liu<sup>b</sup>, Zhenguo Lu<sup>b</sup>, Karin Hinzer<sup>a</sup>

<sup>a</sup>SUNLAB, Centre for Research in Photonics, University of Ottawa, Ottawa, ON, K1N 6N5, Canada

<sup>b</sup>National Research Council Canada, Ottawa, ON, Canada

## ABSTRACT

The emission wavelength of self-assembled quantum dashes can be controlled by their height. Uncapped InAs/InGaAsP/InP quantum dashes are found to have two distinct heights, which we have measured with atomic force microscopy and denoted the plateau and the peak heights. These heights range from 0.50 nm to 2.35 nm. Under the same growth conditions, for increasing uncapped quantum dash heights we observe an increase in the photoluminescence peak emission wavelength from approximately 1535 to 1543 nm for the capped layers. A growth temperature of 520°C is determined to achieve uniform height distribution for 1550 nm emission using chemical beam epitaxy.

**Keywords:** quantum dot, quantum dash, quantum dash laser, atomic force microscopy, emission wavelength, epitaxy, Stranski-Krastanow growth

## 1. INTRODUCTION

Quantum dashes are short wire-like nanoparticles providing three-dimensional electron confinement that can be grown via the Stranski-Krastanow growth mode. The process of self-assembly using this mode for InAs quantum dots was first published in 1985 by Goldstein *et al.* [1]. This layer-plus-island growth, known as Stranski-Krastanow growth, is spontaneous due to the balance between surface energy and strain energy of the InAs layer [2], and requires a significant difference in lattice parameter between the substrate and the layer being grown. The growth mode is characterized by the initial two-dimensional growth of a wetting layer, a highly strained layer a few monolayers thick. After reaching critical thickness, islanding begins on top of the wetting layer to reduce the overall elastic energy of the system. InAs islanding is known to occur on both InP and InGaAsP and will preferentially form dashes or dots depending on the growth conditions. By capping these nanoparticles after self-assembly, quantum dash or dot arrays can be grown in stacks. These stacked arrays offer favourable properties as gain media in lasers compared to quantum wells when used to create multiwavelength lasers for high speed telecommunications [3]. Self-assembled InAs quantum dashes grown on InP substrates can be designed to emit at 1550 nm, in the C-band transmission band of optical fiber.

In this article, four InAs quantum dash samples are analyzed using atomic force microscopy (AFM) to determine the heights of uncapped surface dashes and the effect of growth procedures on dash formation. The method used to extract the heights of these uncapped dashes using open-source software is described, and the relationship between height of dashes and emission wavelength is established. Analyzing these samples yields valuable structural information to understand the confined electronic energy levels within these particles. This data has been used in single quantum dash simulations, which can in turn inform future growth processes and simulations for quantum dash lasers.

## 2. GROWTH OF QUANTUM DASH SAMPLES

### 2.1 InAs/InP self-assembled nanoparticles

InAs quantum dashes on InP substrates are grown by chemical beam epitaxy (CBE). The lattice parameter of InAs is 3.2% larger than InP, and thus Stranski-Krastanow growth readily occurs. As InAs is deposited on (001) InP the 2D to 3D transition occurs through the creation of elongated wire-like structures in the [01-1] direction [4]. With widths much shorter than their lengths, up to hundreds of nanometres, these wire-like nanoparticles are referred to as quantum dashes [4].

\*robhi011@uottawa.ca – SUNLAB – University of Ottawa, Ottawa, ON, Canada

Provided adequate growth interruption times, these dashes can separate into quantum dots with approximately equal lengths and widths. Other factors that affect InAs nanoparticle formation are the group V (As) overpressure, growth temperature, and surface orientation [4][5][6]. Approximately 2-5 monolayers of InAs form as the wetting layer [4]. Uncapped InAs quantum dots grown on InP substrates range from 5-15 nm tall depending on growth procedure and conditions, with widths from 15-40 nm and lengths upwards of 130 nm [4][7]. Quantum dashes can also exhibit taller peaks at the ends of the wires due to diffusion of material during growth interruption and sample cool down. When capped with InP to control their heights, buried InAs quantum dots exhibit heights typically ranging from 1.5-3 nm [4][8]. InAs dashes capped with InGaAsP have been reported with heights of approximately 2 nm [7][6][9][10]. Thin GaAs sublayers have also been deposited prior to the InAs wetting layer to encourage dash growth over dot formation [4]. InAs/InP quantum dot surface densities have been reported as high as  $1 \times 10^{11} \text{ cm}^{-2}$  [4][11]. Heights and densities for InAs dashes on (100) InP substrates with varying buffer layer materials have been reported ranging from 0.4 to 3.1 nm and  $10^9 - 10^{10} \text{ cm}^{-2}$ , respectively [11].

## 2.2 Growth procedure of stacked InAs/InGaAsP/InP quantum dash samples

The quantum dash samples used in this study were grown by CBE with a Riber 32P reactor on n-type (001) InP substrates and consist of five stacks of quantum dash layers with the top layer left uncovered. The growth begins with deposition of an InP buffer followed by an InGaAsP quaternary lattice-matched to InP and emitting at 1.15  $\mu\text{m}$  during room temperature photoluminescence measurements. After the InGaAsP layer a thin GaAs sublayer is grown to promote dash formation over dot formation. InAs is then deposited to form the dashes using a low As overpressure, followed by a 20 second annealing step to allow some ripening of the dashes. The resulting structure after self-assembly is an InAs wetting layer with InAs dashes on top. InP is then used to encase the dashes in a double capping procedure involving a growth interruption between two deposition stages [4]. The InP fills the volume between the dashes, immersing the structures in InP, and the growth interruption serves to control the height distribution of buried dashes by allowing As/P exchange. The exact thickness of the wetting layer after capping is unknown, since As/P exchange will cause InP to form from the InAs wetting layer [4]. After dashes are capped with InP, an InGaAsP barrier is used again to vertically separate each layer of quantum dashes. The fifth and final quantum dash layer is left uncapped on the surface of the samples and was analyzed using AFM. A visual description of the samples is shown in Figure 1. For each sample the dash and barriers layers were grown at a different temperature ranging from 510°C to 540°C, modifying the dash formation and dimensions.

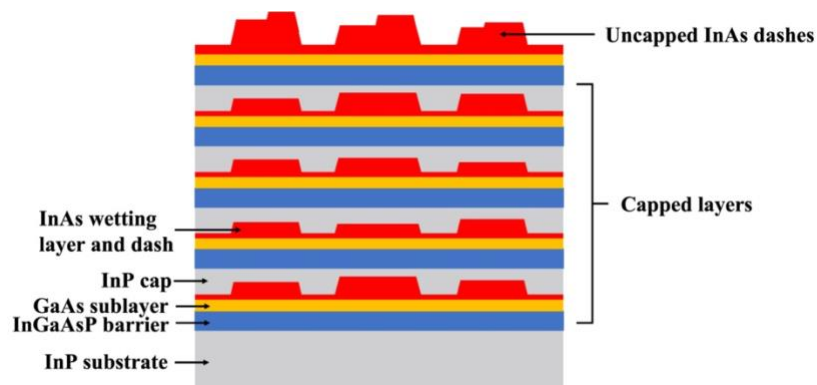


Figure 1. Description of layer structure for quantum dash samples with four capped layers and one uncapped dash layer at the sample surface. Grey: InP substrate and capping layers, blue: InGaAsP barrier layers, yellow: GaAs sublayer, red: InAs wetting layers and dash layers.

### 3. STRUCTURAL ANALYSIS OF QUANTUM DASH SAMPLES

#### 3.1 Measurement and analysis approach

Atomic force microscopy measurements performed using a Bruker Dimension Icon AFM were used to analyze the uncapped InAs quantum dash samples. Four scans at different regions of the sample separated by millimetres were taken to enable averaging that will better characterize the entire sample. Examples of one image taken for each sample are shown in Figure 2. The outer edge of the substrate was avoided since morphology and dash density is impacted by proximity to the edge. The scan conditions are outlined in Table 1.

Table 1. Parameters used for AFM image capture

AFM Parameter	Details
Scan edge size	1 $\mu\text{m}$
Scan resolution	1024 $\times$ 1024
Scan rate	0.5 Hz
AFM Mode	Tapping (ScanAsyst)
AFM cantilever	ScanAsyst-Air tips: silicon nitride triangular cantilevers
Nominal tip radius	2 nm

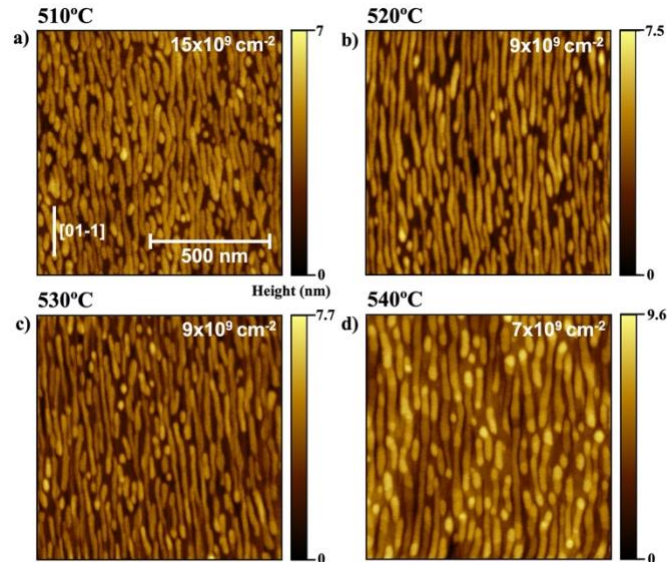


Figure 2. Example AFM images of each quantum dash sample at a) 510°C, b) 520°C, c) 530°C, d) 540°C. Images are 1  $\mu\text{m}^2$  and direction of dash elongation is indicated. Approximated dash densities are listed at the top right of each image.

All AFM images were analyzed using the same process in the open-source software Gwyddion [12]. Data was levelled using mean plane subtraction and a first order polynomial was used to remove linear slopes and arrange each scan line to the same height. The minimum data points were then shifted to zero to establish a baseline. Approximated dash densities were extracted by examining four out of the sixteen AFM images, yielding densities of 7 – 15  $\times 10^9 \text{ cm}^{-2}$  which is on the order of literature values for dash densities and lower than InAs/InGaAsP/InP dot densities [11][4].

Height distributions were extracted from each scan using the one-dimensional statistical function and then fitted using a three-term Gaussian. An example distribution and the corresponding Gaussian terms are shown in Figure 3a, where  $\rho$  is the probability density such that  $\int_{-\infty}^{\infty} \rho(h)dh = 1$  where  $h$  is the height [12]. The first Gaussian term (I) represents the average height distribution of the background area between dashes, which corresponds to the surface roughness of the wetting layer; the second term (II) is the average height distribution of the plateau of the dashes; and the third term (III) is the average height distribution of the local peaks on the dashes arising due to material accumulation at the ends of the dashes during the self-assembly growth process. These three regions are labelled in an example AFM scan in Figure 3b and illustrated diagrammatically in Figure 3c. To determine the mean plateau and peak dash heights of a single scan, the difference between the Gaussian maxima of terms (II) and (I), and (III) and (I) were taken, respectively.

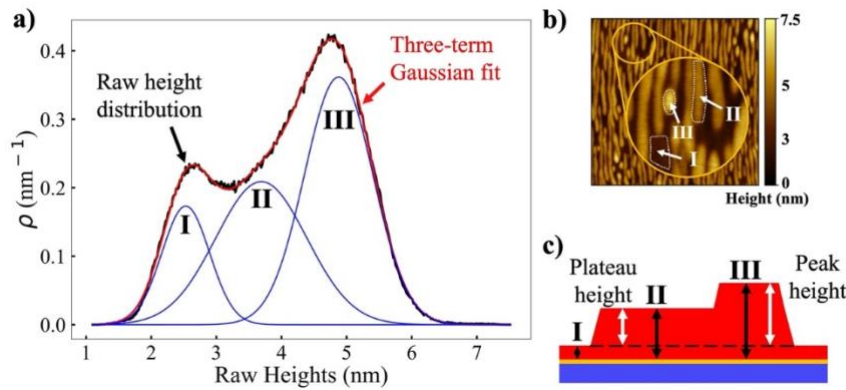


Figure 3. a) Black curve: raw height distribution of single AFM image; red curve: three-term Gaussian fit of raw height distribution; blue curves: individual three Gaussian terms extracted from red curve; b) AFM image with labels corresponding to each height region of the sample; c) visual representation of side profile of surface quantum dash, white arrows indicate dash plateau height and peak dash height.

### 3.2 Growth temperature and dash height

Measurements demonstrate that varying the growth temperature from 510 to 540°C causes variations in the peak dash height of almost 0.5 nm. Table 2 lists the plateau and peak heights for each sample averaged from four scans. Figure 4 graphically represents the average (a) plateau and (b) peak heights in grey, with black error bars corresponding to the maximum and minimum values from the four scans. The plateau height has larger variations between each scan on a single sample surface. As growth temperature reaches 540°C, the average plateau height decreases by approximately 0.5 nm and the surface density of dashes is low compared to other growth temperatures. From Figure 4 we see that the optimal temperature range to grow dashes with the least height variation across four scans is 520°C. This is desirable since the height is used to tune the emission wavelength, and dash layer uniformity is associated with increased optical gain [13].

Table 2. Growth temperature for quantum dash samples with GaAs sublayer and average heights of uncapped dashes

Temperature (°C)	Average Plateau Height (nm)	Average Peak Height (nm)
510	1.14	2.13
520	1.42	2.35
530	1.24	2.10
540	0.50	1.89

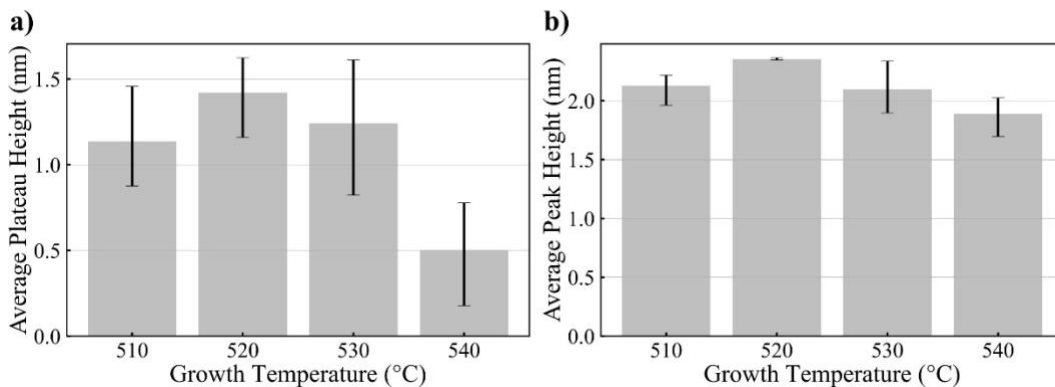


Figure 4. Graphical representation of a) average plateau heights and b) average peak heights of uncapped InAs/InGaAsP/InP quantum dashes. Grey bars indicate average value of height from four different images, and error bars indicate maximum and minimum heights across the four images.

### 3.3 Plateau height and emission wavelength

The lateral dimensions of these quantum dashes are much larger than their heights, therefore energy confinement primarily occurs in the growth direction and determines the nanostructure emission wavelengths [4]. The room temperature photoluminescence emission wavelengths of the four samples are shown in Figure 5a. A growth temperature of 520°C yields the tallest peak and plateau dashes and also corresponds to the emission wavelength closest to the target 1550 nm range. We observe that the relationship between plateau heights and room temperature photoluminescence emission wavelength of the capped dashes is linear for the samples considered. This is shown in Figure 5b.

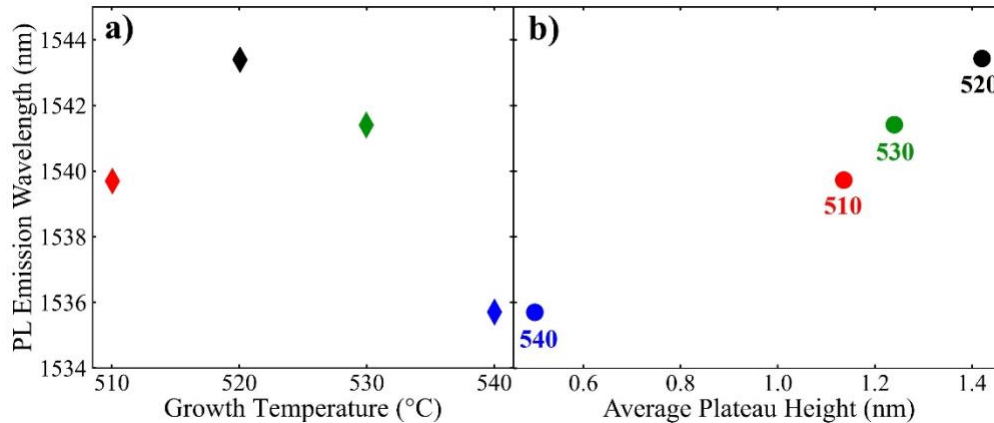


Figure 5. Room temperature photoluminescence emission wavelength of capped quantum dash layers a) as a function of growth temperature and b) as a function of average plateau height with temperature indicated for each data point.

## 4. SUMMARY

Uncapped InAs/InGaAsP/InP quantum dashes were investigated by performing image analysis on AFM scans. There are two distinct height regions identified on these nanoparticles using Gaussian fitting, with one Gaussian distribution corresponding to the elongated plateau of the dashes and another to the peak of the dashes that arises due to surface diffusion dynamics. The optimal temperature range in which to grow uniform dashes emitting closest to 1550 nm is found to be 520°C for the samples considered. This corresponds to the tallest dashes of the samples investigated for both plateau and peak heights. Average peak heights range from 1.89 nm to 2.35 nm. Average plateau heights under 540°C are found to range from 1.14 to 1.42 nm. A growth temperature of 540°C is found to noticeably decrease dash density, plateau, and peak heights, and thus emission wavelength. Since quantum dashes break up and collect to form dots in the Stranski-Krastanow growth mode, they are expected to be thinner than quantum dots. These heights are therefore comparable with similar InAs/InGaAsP/InP nanoparticles in the literature [4][7][11]. The capped quantum dashes in these samples are expected to be shorter than the peak heights identified in this paper due to the InP capping process. The average heights of the dashes extracted from these scans are used to inform the dimensions of single quantum dash simulations investigating the effect of quantum dash structure and composition on emission wavelength.

## ACKNOWLEDGEMENTS

The authors acknowledge financial support from the Natural Sciences and Engineering Research Council of Canada (NSERC) CGS-M scholarship program and the Government of Canada through the National Research Council High-Throughput and Secure Networks Challenge Program #CH-HTSN-216.

## REFERENCES

- [1] L. Goldstein, F. Glas, J. Y. Marzin, M. N. Charasse, and G. Le Roux, "Growth by molecular beam epitaxy and characterization of InAs/GaAs strained-layer superlattices," *Appl. Phys. Lett.*, vol. 47, no. 10, pp. 1099–1101,

- 1985, doi: 10.1063/1.96342.
- [2] B. J. Riel, "An introduction to self-assembled quantum dots," *Am. J. Phys.*, vol. 76, no. 8, pp. 750–757, 2008, doi: 10.1119/1.2907856.
- [3] P. J. Poole, Z. Lu, J. Liu, P. Barrios, Y. Mao, and G. Liu, "A Performance Comparison between Quantum Dash and Quantum Well Fabry-Pérot Lasers," *IEEE J. Quantum Electron.*, vol. 57, no. 6, 2021, doi: 10.1109/JQE.2021.3107850.
- [4] P. J. Poole, *InP-Based Quantum Dot Lasers*, 1st ed., vol. 86. Elsevier Inc., 2012.
- [5] K. Yamaguchi, K. Yujobo, and T. Kaizu, "Stranski-Krastanov growth of InAs quantum dots with narrow size distribution," *Jpn. J. Appl. Phys.*, vol. 39, no. 12 A, 2000, doi: 10.1143/jjap.39.11245.
- [6] F. Genz *et al.*, "InAs nanostructures on InGaAsP/InP(001): Interaction of InAs quantum-dash formation with InGaAsP decomposition," *J. Vac. Sci. Technol. B, Nanotechnol. Microelectron. Mater. Process. Meas. Phenom.*, vol. 28, no. 4, p. C5E1–C5E7, 2010, doi: 10.1116/1.3456173.
- [7] A. Lenz *et al.*, "Formation of InAs/InGaAsP quantum-dashes on InP(001)," *Appl. Phys. Lett.*, vol. 95, no. 20, pp. 108–111, 2009, doi: 10.1063/1.3265733.
- [8] C. Paranthoen *et al.*, "Height dispersion control of InAs/InP quantum dots emitting at 1.55  $\mu\text{m}$ ," *Appl. Phys. Lett.*, vol. 78, no. 12, pp. 1751–1753, 2001, doi: 10.1063/1.1356449.
- [9] M. J. R. Heck *et al.*, "Passively mode-locked 4.6 and 10.5GHz quantum dot laser diodes around 1.55 $\mu\text{m}$  with large operating regime," *IEEE J. Sel. Top. Quantum Electron.*, vol. 15, no. 3, pp. 634–643, 2009, doi: 10.1109/JSTQE.2009.2016760.
- [10] S. C. Heck *et al.*, "Experimental and theoretical study of InAs/InGaAsP/InP quantum dash lasers," *Int. J. Refract. Met. Hard Mater.*, vol. 45, no. 12, pp. 1508–1516, 2009, doi: 10.1109/JQE.2009.2020814.
- [11] M. Z. M. Khan, T. K. Ng, and B. S. Ooi, "Self-assembled InAs/InP quantum dots and quantum dashes: Material structures and devices," *Prog. Quantum Electron.*, vol. 38, no. 6, pp. 237–313, 2014, doi: 10.1016/j.pquantelec.2014.11.001.
- [12] P. Klapetek, D. Nečas, and C. Anderson, "Gwyddion User Guide (gwyddion.net/documentation/user-guide-en)," 2021.
- [13] P. J. Poole *et al.*, "Narrow linewidth 1.52  $\mu\text{m}$  InAs/InP quantum dot DFB lasers," *Conf. Proc. - Int. Conf. Indium Phosphide Relat. Mater.*, vol. 1, pp. 3–6, 2011.